NASA TN D-1582

TECHNICAL NOTE

D-1582

EFFECT OF SURFACE ENERGY ON THE LIQUID-VAPOR INTERFACE CONFIGURATION DURING WEIGHTLESSNESS

By Donald A. Petrash, Thomas M. Nelson, and Edward W. Otto

Lewis Research Center
Cleveland, Ohio

NATIONAL AERONAUTICS AND SPACE ADMINISTRATION
WASHINGTON

January 1963

NATIONAL AERONAUTICS AND SPACE ADMINISTRATION

TECHNICAL NOTE D-1582

EFFECT OF SURFACE ENERGY ON THE LIQUID-VAPOR INTERFACE CONFIGURATION DURING WEIGHTLESSNESS

By Donald A. Petrash, Thomas M. Nelson,
and Edward W. Otto

SUMMARY

As a part of the overall study of the behavior of rocket-engine propellants stored in space-vehicle tanks while exposed to weightlessness and solar and planetary radiant heat sources, an analytical and experimental investigation was conducted to determine the effect of surface energy on the liquid-vapor interface configuration during weightlessness.

An experiment with a capillary tube geometry verified the contention that the solid-liquid-vapor system tends to a configuration in which the free-surface energies are a minimum. This energy minimization process can significantly alter the liquid-vapor interface configuration depending on the geometry employed.

The effect of using a capillary tube as a surface-tension baffle in a spherical and a cylindrical tank on the zero-gravity equilibrium liquid configuration was such that the liquid was positioned in the lower portion of the tank with the vapor located at the top of the tank.

INTRODUCTION

The NASA Lewis Research Center is currently conducting a study of the behavior of rocket engine propellants stored in space-vehicle tanks while exposed to weightlessness (zero gravity) during coasting periods. A part of this program is a study of the liquid-vapor interface configuration under the conditions of weightlessness. The experimental results reported in reference 1 for mercury and alcohol in spheres are the initial effort in this program. The interface configurations observed verified those calculated by Benedikt (ref. 2), Reynolds (ref. 3), and others.

Although the experimental results (ref. 1) indicate that the interface configuration can be predicted for simple containers given the contact angle and ullage volume, the location of this interface is often undesirable from the

standpoint of reliable pumping and venting. This is especially true for a wetting liquid (typical of most propellants currently being considered) in spherical or nearly spherical tanks, because the location of the vapor bubble is random. This creates a venting problem and possibly the problem of aspiration of the bubble into the pump during engine starting. The liquid and vapor could, of course, be properly positioned by acceleration fields produced by such means as a spinning tank or accelerating (ullage) rockets, but these methods require relatively high energy levels or are otherwise undesirable, especially for large vehicles. More desirable would be the proper employment of the surface-tension properties of the liquid itself, possibly through proper tank geometry, as suggested by the dependence of the interface configuration on the contact angle.

Most investigators in the field of capillarity and zero-gravity behavior have suggested that the system tends to assume a condition of minimum energy. The experiments of reference 1 appear to verify this contention because in all cases the liquid-vapor surface tended toward a configuration in which the total energy of the system, considering all areas and unit surface energies, was a minimum. When local minimums were encountered, the system often stabilized at these points. It therefore appeared promising to study the ability of tank geometries providing appreciable changes in surface energy to position the liquid and vapor in acceptable configurations.

A simple configuration that probably has occurred to most investigators in the field and has been suggested and analyzed by Reynolds (ref. 3) is a tube suspended somewhat down from the top of a cylindrical tank concentric with the vertical axis and having an open top and an open bottom. An analysis using either surface energy or capillary pressure drop can be made which shows that a wetting liquid should rise in the tube when the tube diameter is less than one-half the diameter of the tank and fall if it is greater than one-half the tank diameter.

This geometry was considered an excellent one with which to study the interface positioning ability of a tank geometry and to provide further verification of the minimum-surface-energy principle and its usefulness in predicting the interface configuration for geometries in which the contact-angle and ullage-volume methods would fail. This report presents the results of experiments in which the direction of liquid motion depending on the ratio of tube to tank diameter was observed, the velocity of liquid motion was correlated with system dimensions and constants, and the interface configurations were observed in models of spherical and cylindrical propellant tanks with capillary-tube-type surface-tension baffles.

APPARATUS AND PROCEDURE

One of the most direct methods available for producing a weightless environment is that in which a test body undergoes a free fall. During the time in free fall the body is in true weightlessness since there are no restraining forces acting on it.

Test Facility

The weightless environment for this investigation was obtained in a drop tower with a useable drop height of 85 feet that yields a free-fall time of 2.3 seconds. A photograph of the drop tower is presented in figure 1. Air drag on the experiment package was kept to a minimum (less than 10^{-5} g) by allowing it to fall within a protective drag shield. The experiment package and drag shield were unguided during the free fall. A complete description of the test facility is given in reference 1. In this investigation a 2.25-second period of weightlessness was obtained, which is a slight increase over that reported in reference 1. This increase resulted from minor modifications to the drag shield, which reduced the effect of air drag and increased the relative distance between the experimental package and the drag shield.

Experimental Package

The liquid under investigation was contained in glass tanks suitably mounted to allow a high-speed motion picture camera to photograph the entire assembly during the free fall. A photograph of the experimental package is presented in figure 2.

Three tank geometries were investigated in this experimental study. The capillary investigation was conducted with a glass tube mounted concentrically inside a cylindrical glass tank. The tube was supported by a Lucite clamp suspended from the top of the tank. Six capillary tubes having different diameters were investigated. A sketch of the tank geometry and pertinent dimensions are presented in figure 3. The liquid-positioning investigation was conducted by using a 100-milliliter glass sphere and a 440-milliliter glass cylinder. A standpipe (capillary tube) capable of containing 15 percent of the volume of the tank was mounted inside each tank. Holes were drilled in the base of the standpipe to allow liquid to flow between the standpipe and the tank. A sketch of the two tank geometries is presented in figure 4.

Test Liquid

The liquid used in this investigation was 200-proof ethyl alcohol. This liquid is representative of a totally wetting liquid. The properties of ethyl alcohol that are pertinent to this investigation are given in appendix B. During the experimental investigation, the test liquid was at essentially ambient pressure and temperature. The liquid-vapor interface was liquid to air. A small amount of blue dye (methylene blue) was added to the alcohol to improve the photographic quality. The addition of the dye had no measurable effect on the surface tension of the alcohol.

Operating Procedure

The operating procedure used in this investigation was essentially the same as that discussed in reference 1, with the following exception. The glass tanks and associated glassware used in handling the test liquid were cleaned ultrasonically in a solution of detergent and distilled water, rinsed in distilled water, and dried in a warm air dryer.

RESULTS AND DISCUSSION

Capillary Investigation

The results of the experimental investigation of ethyl alcohol in tubes 0.48, 1.10, 2.20, 3.40, 4.60, and 5.90 centimeters in diameter mounted in a 6.90-centimeter-diameter tank are shown in figures 5 and 6 in the form of selected frames from the motion pictures obtained during each test drop. For each of these tube sizes and for each volume of liquid investigated, three photographs are presented. The first shows the liquid configuration prior to being subjected to zero gravity. The second shows the liquid as it is rising in the capillary space. The third shows the liquid at the maximum capillary-rise height obtainable in the test apparatus as limited either by experimental test time or system geometry.

Direction of liquid motion. - It can be observed in figures 5(a) to (i) that, for the 0.48-, 1.10-, and 2.20-centimeter-diameter tubes, the capillary liquid rise occurs in the tube. The radii of these three tubes are less than one-half the radius of the cylindrical tank. The results obtained for the 3.40-centimeter-diameter tube are shown in figure 5(j) and indicate that, when the radius of the tube is equal to one-half the radius of the tank, no capillary rise occurs. When the radius of the tube is increased so that it is larger than one-half the radius of the tank, the capillary liquid rise occurs in the annular space. The results obtained in the 4.60- and 5.90-centimeter-diameter tubes are presented in figure 6 and illustrate the annular capillary rise. The experimental results presented in figures 5 and 6 agree with the analysis of appendix B as to the effect of tube diameter on the direction of capillary rise (eqs. (B1) and (B9)). They also provide further experimental verification of the tendency of the liquid-vapor-solid system to assume a configuration in which the total surface energy is a minimum.

Time response of liquid rise. - The variation of the height of the liquid in the capillary tubes with time in zero gravity is presented in figure 7 for tube diameters of 0.48, 1.10, and 2.20 centimeters and for a range of initial heights l_t. These data were obtained from an analysis of the motion pictures taken during the experimental study. The solid lines are analog computer solutions of the equation

$$\ddot{Z} = \frac{\frac{2\sigma_{lv}\cos\theta}{\rho}\left(\frac{1}{r} - \frac{1}{R - r}\right) - \frac{1}{2}K\dot{Z}^2 - \frac{8\nu(l_t + Z)}{r^2}\dot{Z}}{\left(1 - \frac{A_t^2}{A_a^2}\right)Z + l_t + \frac{A_t}{A_c}l_c + \frac{A_t}{A_a}l_a} \tag{B17}$$

(which is derived in appendix B) for liquid rise as a function of time. (Symbols are defined in appendix A.) Equation (B17) is similar to that employed by many capillary investigators and is derived from a fundamental force-mass relation that accounts for forces due to surface tension, entrance losses, and friction drag as follows:

$$\begin{pmatrix}\text{Surface-}\\\text{tension}\\\text{force}\end{pmatrix} - \begin{pmatrix}\text{Entrance-}\\\text{pressure-}\\\text{loss force}\end{pmatrix} - \begin{pmatrix}\text{Friction-}\\\text{drag}\\\text{force}\end{pmatrix} = \begin{pmatrix}\text{Effective mass}\\\text{of liquid in}\\\text{system}\end{pmatrix}\begin{pmatrix}\text{Acceleration}\\\text{of liquid}\\\text{in tube}\end{pmatrix}$$

This equation involves no empirical constants and can be evaluated from the physical constants of the system with the exception of a constant applied to the entrance-loss term, which is calculated by approximate means. In the solutions shown in figure 7 this constant was taken as 2.28, as calculated in reference 4. The system constants used in obtaining the solution of figure 7 are given in appendix B.

The correlation of the data with the analysis is satisfactory for variations in tube diameter and for variations in initial height of liquid. The degree of correlation does indicate that equation (B17) incorporates the principal physical phenomena and is useful for calculating the velocities and displacements in capillary systems in zero gravity.

The variation of the height of rise of the liquid in the annular space with time in zero gravity is presented in figure 8 for the 5.10- and 6.40-centimeter-diameter tubes. The solid lines are an analog computer solution of equation (B17) using the appropriate system dimensions and a value for the velocity-entrance-loss coefficient K of four times that used for the solutions in figure 7. No attempt was made to calculate the value of K that would apply to the annular configuration. Here again the correlation with varying tube diameter is good, which indicates that equation (B17) incorporates the principal physical phenomena and that it would be useful for calculating the velocities and displacements in capillary systems in zero gravity.

Applications

The results obtained from the experimental investigation of the capillary phenomena indicate the possibility of using the principle of minimum surface energy to position the liquid in a space-vehicle propellant tank in a desirable location. An experimental investigation was therefore conducted to determine

the effectiveness of using a capillary tube to locate the liquid in a spherical and a cylindrical tank. It is realized that a multitude of internal geometries could be considered for liquid-vapor locators. It is felt, however, that the shape chosen herein is a simple design that illustrates the fundamental principle. The capillary tubes or standpipes were designed so that the capillary liquid rise would occur in the tube and not in the annular space. The results are presented in the form of selected frames taken from the motion pictures obtained during each test drop. The photographs generally show the 1-g liquid configuration, the liquid as it rises in the standpipe, and the zero-g equilibrium liquid configuration.

Sphere with standpipe. - The photographs obtained from the experimental investigation of ethyl alcohol in a 100-milliliter sphere with a standpipe, over a range of liquid- to tank-volume ratios, are presented in figure 9. It is observed that in all cases the standpipe had a significant influence on the configuration of the liquid in the tank as compared with the liquid configuration in a sphere with no internal tank baffles reported in reference 1. At a liquid- to tank-volume ratio of 10 percent the liquid rose in the standpipe until the ports at the base of the standpipe became uncovered. At that time the liquid rise stopped because the forces, energies or pressure drops, causing the liquid rise in the standpipe became balanced, and the liquid remained in the standpipe for the remainder of the test. At liquid- to tank-volume ratios of 20 to 50 percent the liquid rose in the standpipe until it became full. The remaining liquid in the tank was located in the lower hemisphere of the tank. At liquid- to tank-volume ratios of 70 and 90 percent the liquid configuration was a full standpipe with a vapor bubble inside the liquid. It should be noted that at these volume ratios the vapor bubble did not remain at the top of the sphere but moved down the walls and was finally located between the standpipe and the tank walls. This bubble motion is attributed to a slight misalinement of the axis of the standpipe and the axis of the sphere.

The variation of the liquid rise in the standpipe is plotted against time in zero gravity for liquid- to tank-volume ratios of 20 to 50 percent in figure 10. It is observed that the slope of these data is the rise velocity and that, when the velocities became nearly constant, they were essentially the same value regardless of the amount of liquid in the tank; this indicates that the flow may have been controlled by the holes in the base of the tube.

It can be concluded from this experimental study that a capillary surface-tension baffle (standpipe) is an effective means of positioning the liquid in a spherical tank. In all cases the standpipe was full of liquid during the weightless period and the remainder of the liquid was positioned in the lower hemisphere of the tank. This configuration corresponds to a condition in which the surface energies of the system are at a minimum.

Cylinder with standpipe. - The photographs obtained from the experimental investigation of ethyl alcohol in a 440-milliliter cylinder with a standpipe, over a range of liquid- to tank-volume ratios, are presented in figure 11. At liquid- to tank-volume ratios of 10 to 50 percent, the liquid rose in the

standpipe during the duration of the weightless period. The remaining liquid was located in the lower end of the tank during this period. At a liquid- to tank-volume ratio of 70 percent, the liquid rose in the standpipe and filled the standpipe before the end of the test period. The remaining liquid was located in the lower portion of the tank. At a liquid- to tank-volume ratio of 90 percent, the liquid configuration was that of a full standpipe with a vapor bubble inside the liquid. The vapor bubble remained at the top of the tank above the standpipe for the duration of the weightless period.

The variation of liquid rise in the standpipe is plotted against time in zero gravity for liquid- to tank-volume ratios of 10, 20, 30, 40, 50, and 70 percent in figure 12. It is again noted that the liquid rise velocity was essentially the same regardless of the amount of liquid in the tank, and the spread of the data is attributed to the longer formation times in the cylindrical tank.

It can be concluded from these experimental results that a capillary surface-tension baffle (standpipe) is an effective means of positioning the liquid in a cylindrical tank. In all cases the liquid rose in the standpipe and the remainder was located at one end of the cylinder. This configuration again corresponds to a condition in which the surface energies of the system are at a minimum.

SUMMARY OF RESULTS

The experimental investigation of the capillary phenomena in a weightless environment and its application to control of the position of propellants in space-vehicle propellant tanks yielded the following results:

1. The liquid-vapor interface assumes a configuration corresponding to a condition in which the surface energies of the system were at a minimum. This principle can be used to determine the liquid-vapor interface configuration in a tank of any geometry and to design tank geometries to obtain desired interface configurations.

2. A satisfactory correlation was obtained between the calculated capillary rise as a function of time and the experimental data.

3. The effect of using a capillary tube as a surface-tension baffle in a spherical and a cylindrical tank on the equilibrium liquid configuration was such that the liquid was positioned in the lower portion of the tank and the vapor at the top of the tank.

Lewis Research Center
National Aeronautics and Space Administration
Cleveland, Ohio, September 24, 1962

APPENDIX A

SYMBOLS

A	surface area of annulus, cm^2
A_a	cross-sectional area of annulus, cm^2
A_c	cross-sectional area of connecting passage, cm^2
A_t	cross-sectional area of tube, cm^2
a	surface area of tube, cm^2
F	capillary force in annulus, dynes
f	capillary force in tube, dynes
H	liquid height in annulus, cm
h	liquid height in tube, cm
K	velocity-entrance-loss coefficient (see ref. 4)
l_a	initial length of liquid in annulus, cm
l_c	effective length of liquid in connecting passage, cm
l_e	effective total length of liquid being accelerated, cm
l_t	initial length of liquid in tube, cm
M_e	effective mass of liquid in system, g
P	pressure in annulus immediately inside liquid-vapor interface, $dynes/cm^2$
ΔP	pressure drop, force/area, $dynes/cm^2$
P_a	pressure outside liquid-vapor interface, $dynes/cm^2$
p	pressure in tube immediately inside liquid-vapor interface, $dynes/cm^2$
R	radius of tank, cm
r	radius of tube, cm
S	surface energy in annulus, dynes/cm

s surface energy in tube, dynes/cm

Z height, cm

θ contact angle of liquid against solid, deg

ν viscosity, poise

ρ density, g/cm^3

σ surface tension, dynes/cm

Subscripts:

ls liquid-solid interface

lv liquid-vapor interface

vs vapor-solid interface

Superscripts:

$\cdot$ first derivative with respect to time

$\cdot\cdot$ second derivative with respect to time

APPENDIX B

DERIVATION OF CAPILLARY-RISE DIRECTION AND TIME RESPONSE OF LIQUID RISE FOR A TUBE MOUNTED IN A CYLINDRICAL CONTAINER

Capillary-Rise Direction

The direction of liquid motion in a capillary system such as that shown in figure 3 may be derived from a consideration of either capillary forces or surface energy. Because each method provides insight into behavior of the system, each will be derived.

Capillary-force method. - Figure 13(a), a sketch of a capillary system of the type under consideration, presents a general situation of a liquid with a contact angle θ and shows the forces, pressures, and system radii. If capital letters are used to denote quantities applicable to the annulus and small letters those applicable to the inside of the tube, the following equations may be written for the vertical forces at the solid-liquid-vapor interfaces:

$$f = 2\pi r\sigma_{lv} \cos \theta$$

and

$$F = 2\pi(R + r)\sigma_{lv} \cos \theta$$

(The thickness of the capillary tube is considered to be zero.) The pressure drop across each liquid-vapor interface may be obtained by dividing each equation by the respective area as follows:

$$P_a - p = \frac{2\pi r\sigma_{lv} \cos \theta}{\pi r^2} = \frac{2\sigma_{lv} \cos \theta}{r}$$

and

$$P_a - P = \frac{2\pi(R + r)\sigma_{lv} \cos \theta}{\pi(R^2 - r^2)} = \frac{2\sigma_{lv} \cos \theta}{R - r}$$

The pressure difference tending to drive liquid up or down the tube (P_a is common to both surfaces) is found as follows:

$$(P_a - p) - (P_a - P) = P - p = \frac{2\sigma_{lv} \cos \theta}{r} - \frac{2\sigma_{lv} \cos \theta}{R - r}$$

More simply,

$$P - p = 2\sigma_{lv} \cos \theta \left(\frac{1}{r} - \frac{1}{R - r}\right) \tag{B1}$$

For a wetting liquid ($\theta = 0^\circ$ to 90°) $\cos \theta$ is positive and, by inspection, the following behavior is evident: For $r < R/2$, $P - p > 0$ and the liquid will rise in the tube; for $r = R/2$, $P - p = 0$ and the liquid will neither rise nor fall; for $r > R/2$, $P - p < 0$ and the liquid will fall in the tube. For nonwetting liquids ($\theta = 90^\circ$ to 180°) $\cos \theta$ is negative and thus the pressure drop and consequently the direction of liquid movement in the tube will be reversed.

It is interesting to note that equation (B1) is independent of gravity. Thus the direction of liquid motion is the same in zero gravity as in a gravity field; only the height of the liquid rise is affected by the gravity level.

Surface-energy method. - Although equation (B1) adequately describes the direction of fluid motion, a better insight into the energy relation is obtained by deriving the relation for fluid movement in terms of the surface energies. Figure 13(b) is a sketch of the capillary system under consideration and shows the applicable surface energies and system dimensions. Consider a change in liquid height in the tube Δh. The change in energy on the inside tube surface Δs will equal the gain in energy due to covering the area Δa with liquid minus the loss in energy due to the loss in vapor wetted area:

$$\Delta s = \Delta a\, \sigma_{ls} - \Delta a\, \sigma_{vs} = \Delta a(\sigma_{ls} - \sigma_{vs}) \tag{B2}$$

The values of the quantities σ_{ls} and σ_{vs} are unknown; however, they are related to the surface energy of the liquid and the contact angle by the Young-Dupre equation:

$$\sigma_{vs} - \sigma_{ls} = \sigma_{lv} \cos \theta \tag{B3}$$

Substituting this expression in equation (B2) gives

$$\Delta s = -\Delta a\, \sigma_{lv} \cos \theta \tag{B4}$$

By a similar process for the annulus (considering an upward rise) the following is obtained:

$$\Delta S = -\Delta A\, \sigma_{lv} \cos \theta \tag{B5}$$

The surface-area changes Δa and ΔA are obtained in terms of the height changes Δh and ΔH, and equations (B4) and (B5) become:

$$\Delta s = -2\pi r\, \Delta h\, \sigma_{lv} \cos \theta \tag{B6}$$

and

$$\Delta S = -2\pi(R + r)\Delta H\, \sigma_{lv} \cos \theta \tag{B7}$$

The annular height change ΔH can be obtained in terms of the tube height change as follows:

$$\Delta H = -\Delta h \frac{r^2}{R^2 - r^2}$$

Substituting this expression in equation (B7) yields

$$\Delta S = 2\pi \frac{r^2}{R - r} \Delta h \, \sigma_{lv} \cos \theta \tag{B8}$$

The total energy change in the system is obtained by adding the energy changes Δs and ΔS as follows:

$$\Delta s + \Delta S = -2\pi r \, \Delta h \, \sigma_{lv} \cos \theta + 2\pi \frac{r^2}{R - r} \Delta h \, \sigma_{lv} \cos \theta$$

When the terms are simplified and collected,

$$\Delta s + \Delta S = -2\pi r^2 \, \Delta h \, \sigma_{lv} \cos \theta \left(\frac{1}{r} - \frac{1}{R - r} \right) \tag{B9}$$

The premise that the liquid-vapor system will seek a configuration of minimum total energy requires that the sum of the energy changes $\Delta s + \Delta S$ be negative. This condition is obtained in equation (B9) if the multiple of Δh, $\cos \theta$, and $\frac{1}{r} - \frac{1}{R - r}$ is positive. The term Δh was taken as positive in the upward direction; thus for $0^\circ < \theta < 90^\circ$ the liquid will rise in the tube if $r < R/2$, remain stationary if $r = R/2$, and fall if $r > R/2$. For $90^\circ < \theta < 180^\circ$ the opposite situation is obtained.

Capillary Rise as Function of Time

The equation for capillary motion in the tube under zero-gravity conditions can be derived from Newton's force-mass relation as follows:

$$\begin{pmatrix}\text{Surface-}\\ \text{tension}\\ \text{force}\end{pmatrix} - \begin{pmatrix}\text{Entrance-}\\ \text{pressure-}\\ \text{loss force}\end{pmatrix} - \begin{pmatrix}\text{Friction-}\\ \text{drag}\\ \text{force}\end{pmatrix} = \begin{pmatrix}\text{Effective mass}\\ \text{of liquid in}\\ \text{system}\end{pmatrix} \begin{pmatrix}\text{Acceleration}\\ \text{of liquid}\\ \text{in tube}\end{pmatrix}$$

If each side is divided by the area of the tube A_t, this equation becomes:

$$\Delta P_{\text{surf ten}} - \Delta P_{\text{vel hd}} - \Delta P_{\text{fric}} = \frac{M_e}{A_t} \ddot{Z} \tag{B10}$$

where M_e is the effective mass of liquid in the system, $\ddot{Z}$ is the acceleration of the liquid in the tube, and the ΔP's are the designated pressure drops.

The expressions for the various pressure drops are written (for the geometry of fig. 13(c)) as follows:

$$\Delta P_{surf\ ten} = 2\sigma_{lv} \cos\theta \left(\frac{1}{r} - \frac{1}{R - r}\right) \tag{B11}$$

$$\Delta P_{vel\ hd} = \frac{1}{2} K\rho\dot{Z}^2 \tag{B12}$$

$$\Delta P_{fric} = \frac{8\rho\nu(l_t + Z)}{r^2} \dot{Z} \tag{B13}$$

where equation (B11) is a form of equation (B1), equation (B12) is a conventional expression for velocity-head loss, and equation (B13) is the Poiseuille expression for friction pressure loss.

The effective mass M_e is expressed as follows:

$$M_e = \rho A_t l_e \tag{B14}$$

where l_e is the effective length of fluid being accelerated at rate $\ddot{Z}$. This effective length is found by adding to the length of liquid in the tube being accelerated at rate $\ddot{Z}$ the other liquid lengths modified by the area ratios to account for their differing acceleration rates as follows:

$$l_e = l_t + Z + \frac{A_t}{A_c} l_c + \frac{A_t}{A_a}\left(l_a - \frac{A_t}{A_a} Z\right) \tag{B15}$$

Substituting this expression in equation (B14) and rearranging give

$$M_e = \rho A_t \left[\left(1 - \frac{A_t^2}{A_a^2}\right) Z + l_t + \frac{A_t}{A_c} l_c + \frac{A_t}{A_a} l_a\right] \tag{B16}$$

Substituting this expression in equation (B10) and solving for $\ddot{Z}$ result in

$$\ddot{Z} = \frac{\frac{2\sigma_{lv} \cos\theta}{\rho}\left(\frac{1}{r} - \frac{1}{R - r}\right) - \frac{1}{2} K\dot{Z}^2 - \frac{8\nu(l_t + Z)}{r^2} \dot{Z}}{\left(1 - \frac{A_t^2}{A_a^2}\right) Z + l_t + \frac{A_t}{A_c} l_c + \frac{A_t}{A_a} l_a} \tag{B17}$$

The velocity and displacement expressions may be obtained by successive integration.

The solutions of this equation for Z as a function of time presented in figures 7 and 8 were obtained using the following values for various properties of alcohol:

Surface tension at vapor-liquid interface, σ_{lv}, dynes/cm	22.3
Contact angle of liquid against solid, θ, deg	0
Density, ρ, g/cm^3	0.789
Viscosity, ν, poise	0.012

The tube and tank radii r and R and the various areas A_t, A_a, and A_c can be obtained from figure 3. The area A_c was taken as a cylindrical area of radius r and height h. The thickness of the tube was taken into account where significant in the calculations for A_a. The initial heights l_t and l_a, which differ only by the 1-g capilliary rise, were calculated from the initial fillings given in figures 7 and 8. The small initial capillary rise in the tube or annulus was disregarded because its effect on the calculations was very small for most cases and because of the uncertainty in estimating the length l_c, which was taken approximately along the path indicated in figure 13(c). The value of K of 2.28 was taken from reference 4 for the case where the tube was less than one-half the tank diameter, and for the cases where the tube was greater than one-half the tank diameter a value four times greater (9.12) was used.

REFERENCES

1. Petrash, Donald A., Zappa, Robert F., and Otto, Edward W.: Experimental Study of the Effects of Weightlessness on the Configuration of Mercury and Alcohol in Spherical Tanks. NASA TN D-1197, 1962.

2. Benedikt, E. T.: General Behavior of a Liquid in a Zero or Near Zero Gravity Environment. Rep. ASG-TM-60-9Z6, Norair Div., Northrop Corp., May 1960.

3. Reynolds, William C.: Hydrodynamic Considerations for the Design of Systems for Very Low Gravity Environments. Rep. LG-1, Stanford Univ., Sept. 1961.

4. Langhaar, H.: Steady Flow in the Transition Length of a Straight Tube. Jour. Appl. Mech., vol. 9, no. 2, June 1942, pp. A-55-A-58.

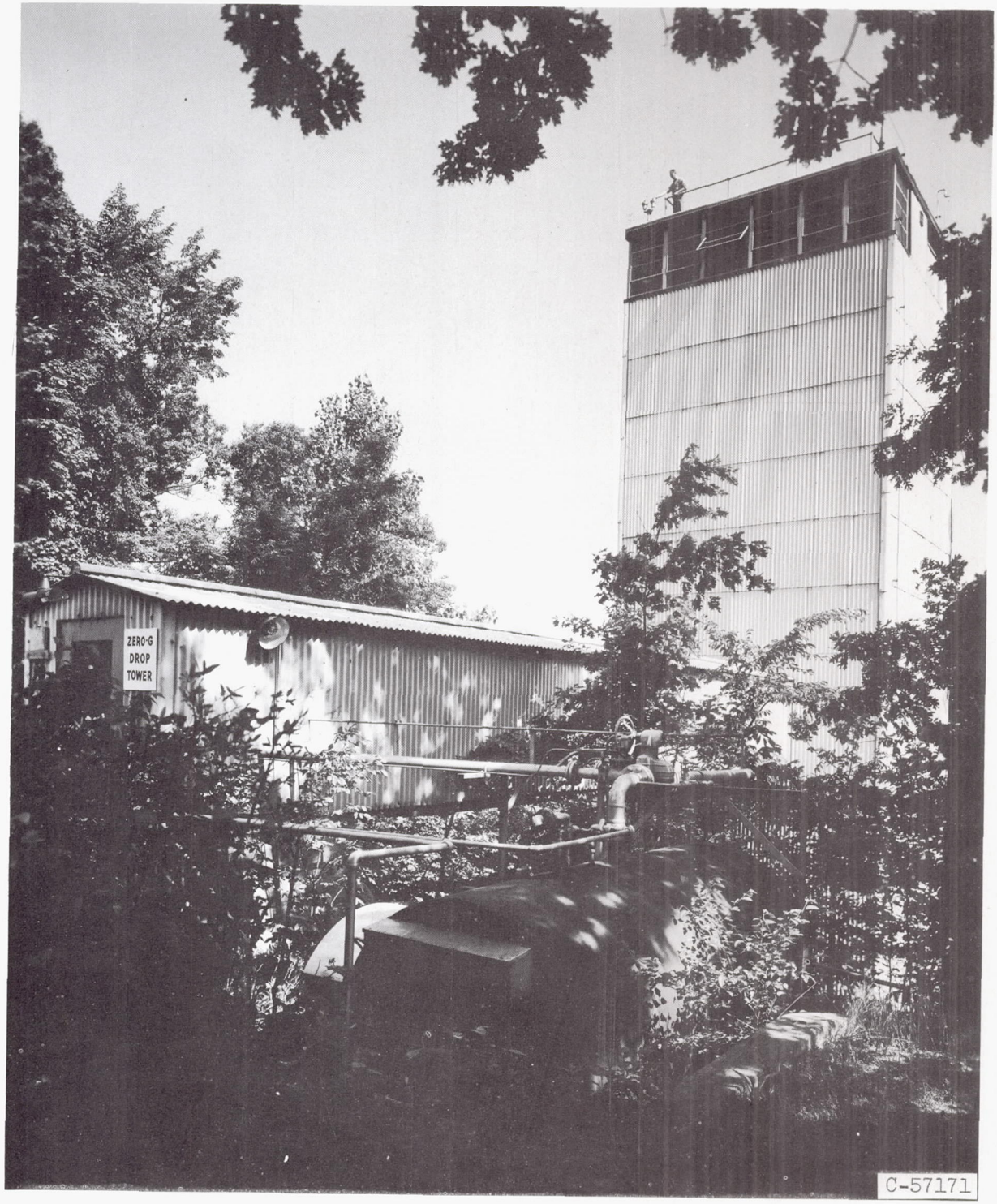

Figure 1. - 100-foot drop tower.

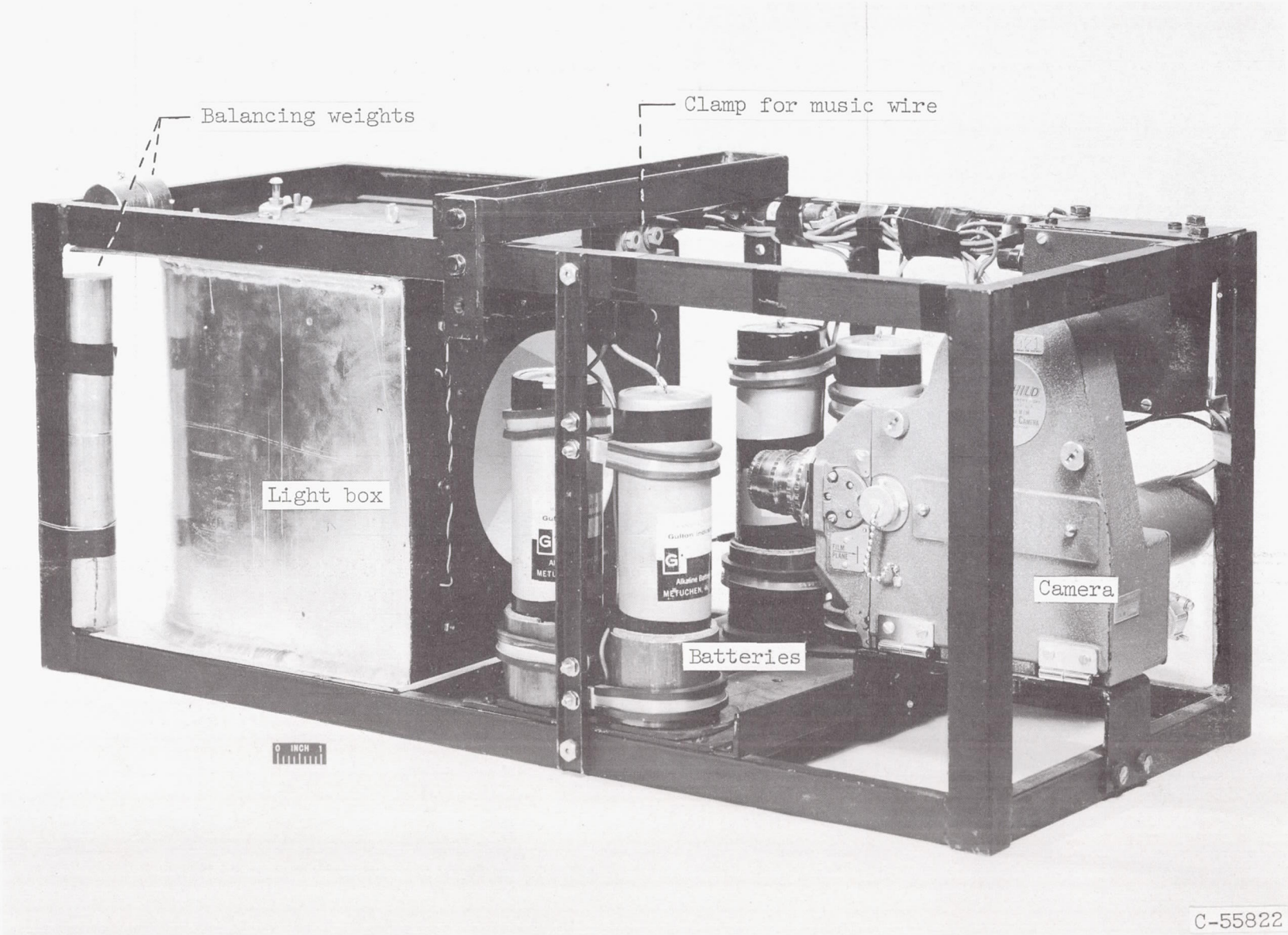

Figure 2. - Experiment package showing camera, batteries, light box, and balancing weights.

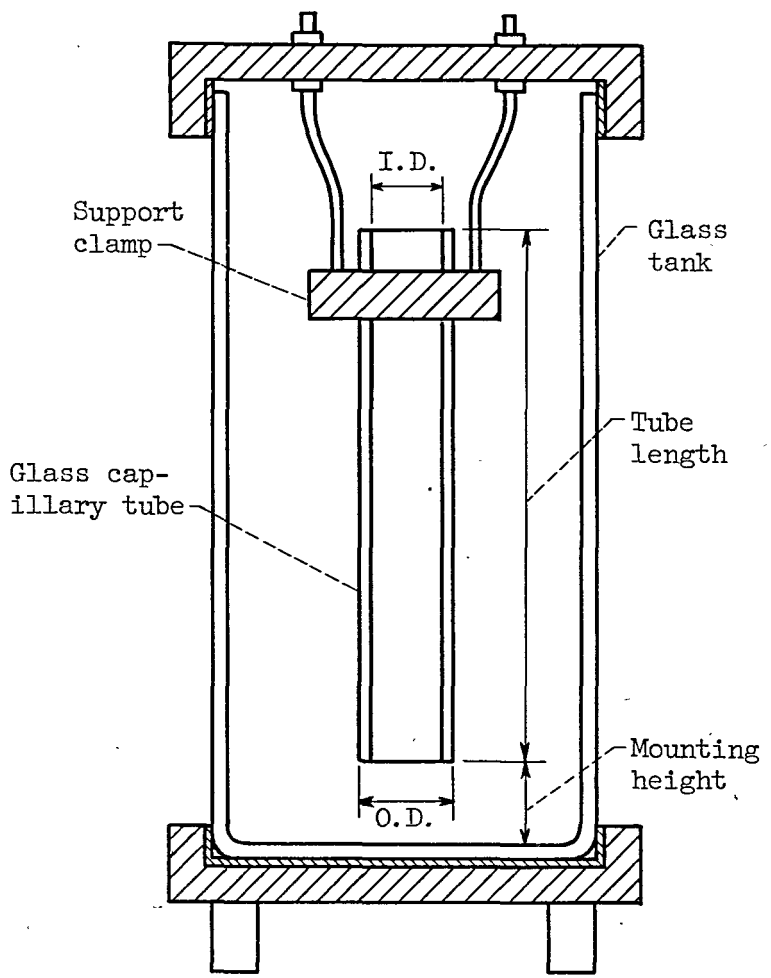

	Inside diameter, cm	Outside diameter, cm	Length, cm	Mounting height, cm
Tank	6.90	7.30	15.20	----
Tube 1	.48	.72	10.51	1.50
Tube 2	1.10	1.30	10.56	1.50
Tube 3	2.20	2.50	10.50	1.50
Tube 4	3.40	3.80	10.54	1.55
Tube 5	4.60	5.10	10.52	.90
Tube 6	5.90	6.40	10.57	.25

Figure 3. - Sketch of capillary-tube configuration showing dimensions.

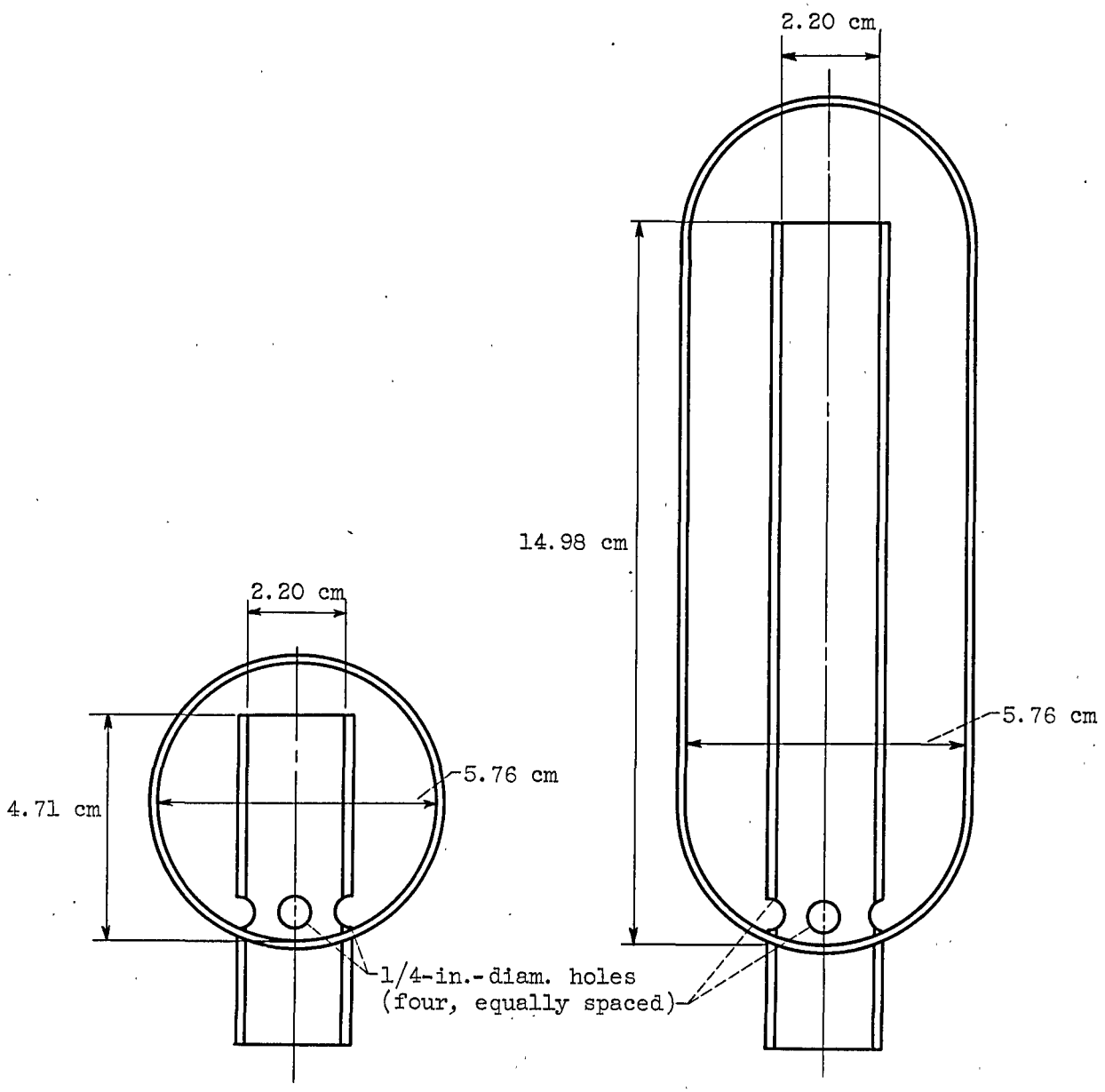

(a) 100-milliliter sphere with standpipe.

(b) 440-milliliter cylinder with standpipe.

Figure 4. - Sketch of spherical and cylindrical tanks with capillary surface-tension baffles.

1-g configuration

Max.-height configuration

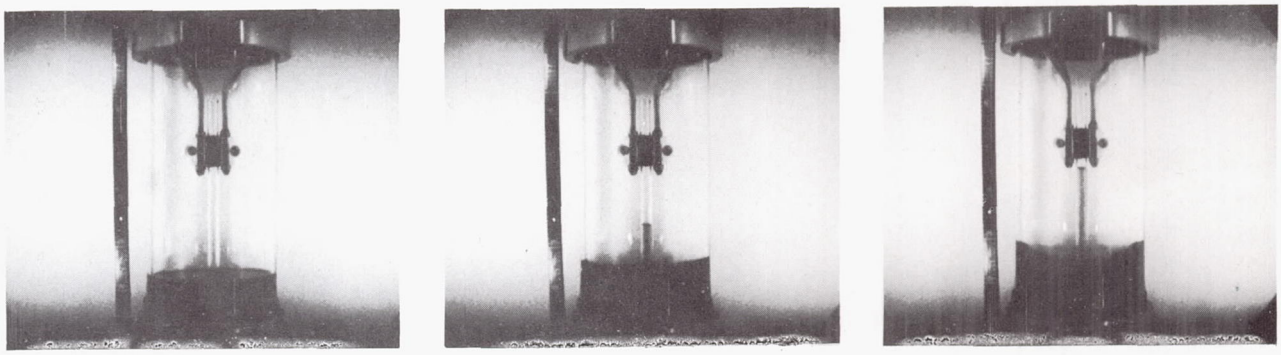

0 sec 0.25 sec 0.58 sec

(a) Tube diameter, 0.48 centimeter; amount of liquid in tank, 70.7 milliliters.

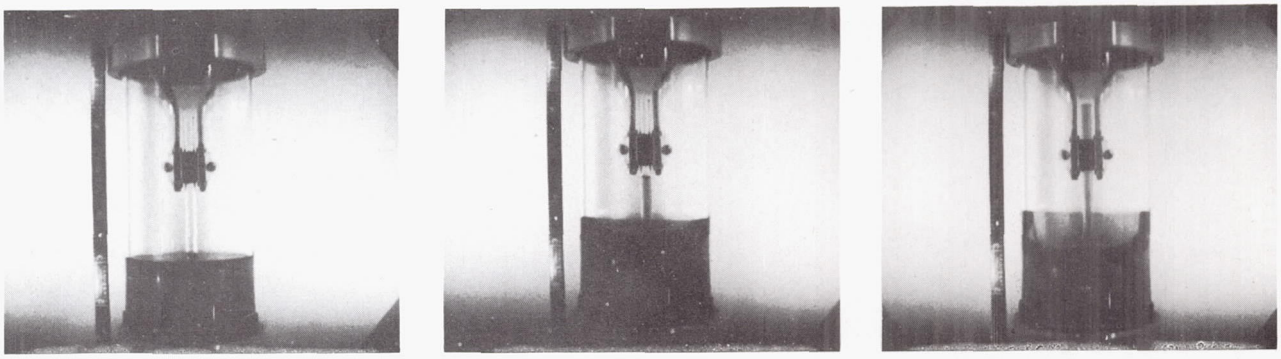

0 sec 0.46 sec 0.99 sec

(b) Tube diameter, 0.48 centimeter; amount of liquid in tank, 144.9 milliliters.

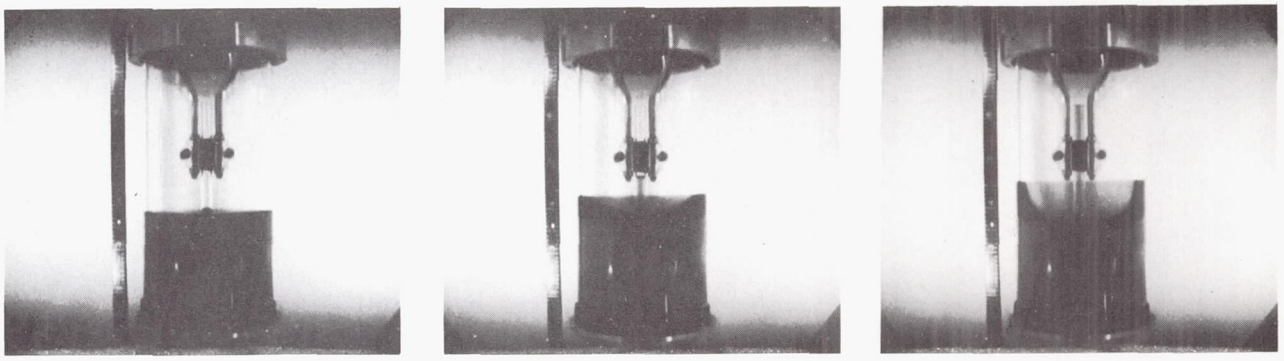

0 sec 0.42 sec 0.91 sec C-61699

(c) Tube diameter, 0.48 centimeter; amount of liquid in tank, 219.1 milliliters.

Figure 5. - Capillary rise in tube.

1-g configuration

Max.-height configuration

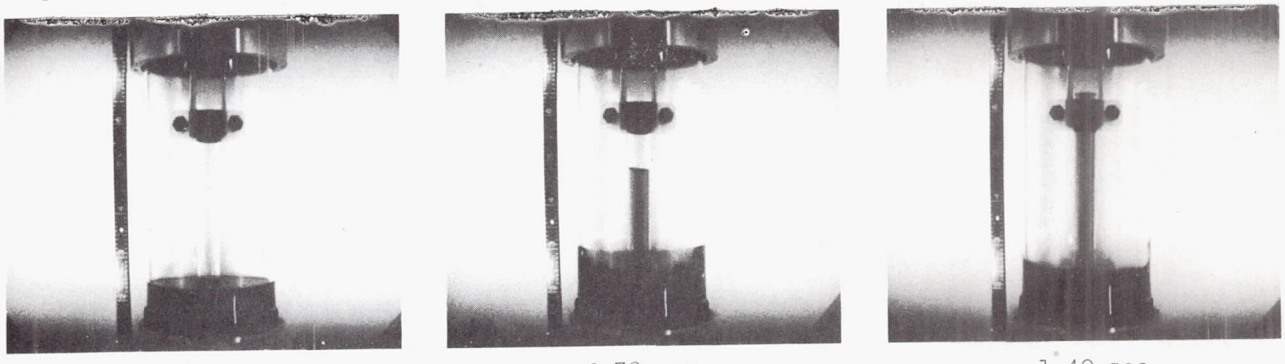

0 sec 0.78 sec 1.40 sec

(d) Tube diameter, 1.10 centimeters; amount of liquid in tank, 77.0 milliliters.

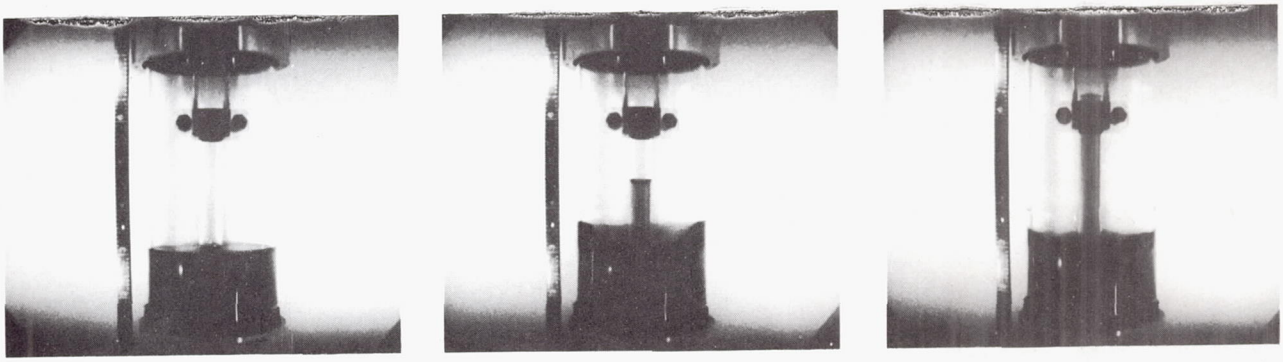

0 sec 0.66 sec 1.31 sec

(e) Tube diameter, 1.10 centimeters; amount of liquid in tank, 149.0 milliliters.

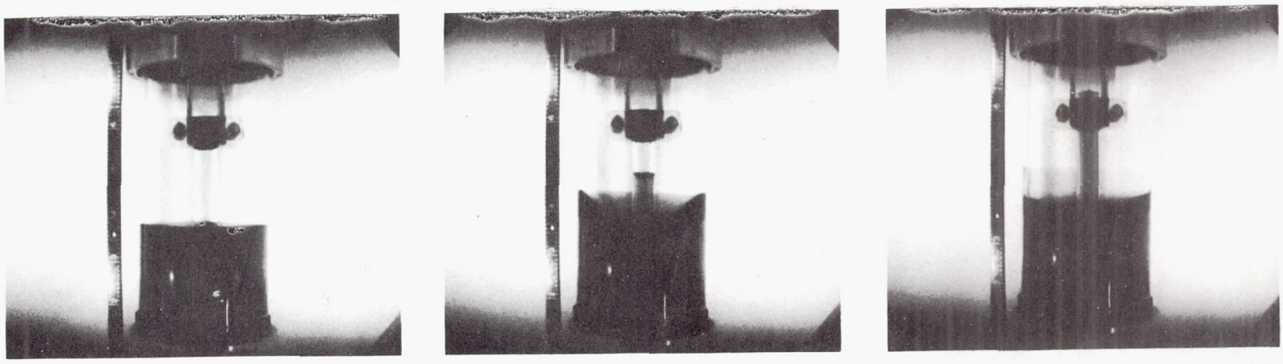

0 sec 0.63 sec 1.27 sec C-61700

(f) Tube diameter, 1.10 centimeters; amount of liquid in tank, 221.0 milliliters.

Figure 5. - Continued. Capillary rise in tube.

1-g configuration

Max.-height configuration

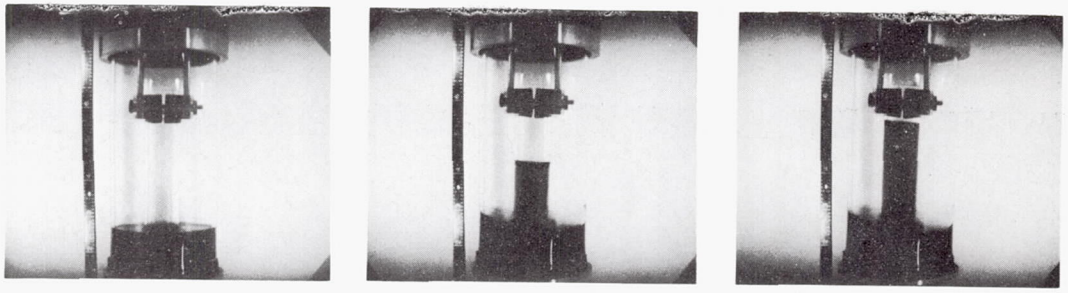

0 sec

1.15 sec

1.73 sec

(g) Tube diameter, 2.20 centimeters; amount of liquid in tank, 103.7 milliliters.

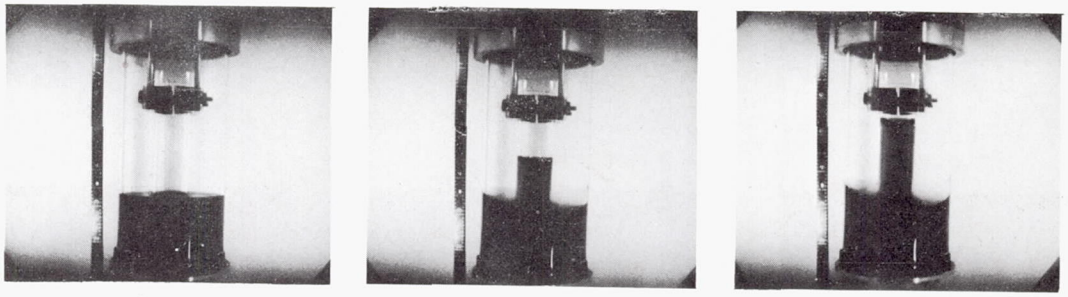

0 sec

1.06 sec

1.57 sec

(h) Tube diameter, 2.20 centimeters; amount of liquid in tank, 168.7 milliliters.

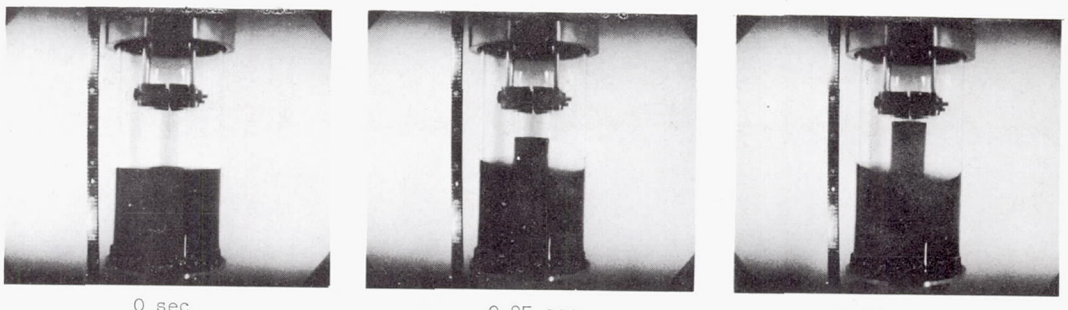

0 sec

0.85 sec

1.30 sec

(i) Tube diameter, 2.20 centimeters; amount of liquid in tank, 233.7 milliliters.

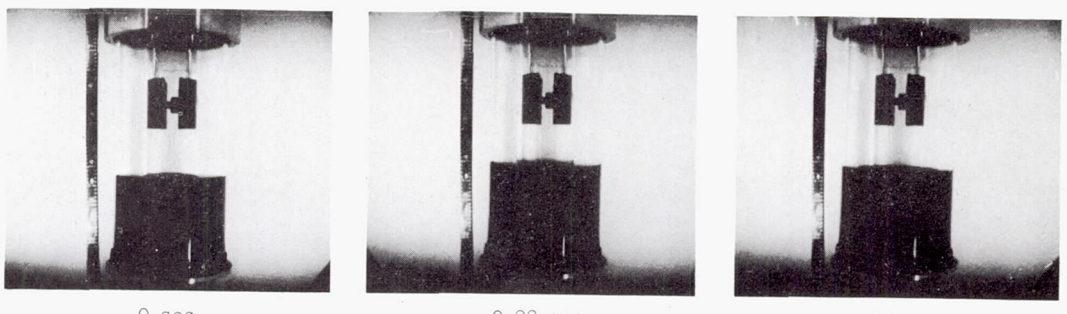

0 sec

0.99 sec

2.22 sec C-61701

(j) Tube diameter, 3.40 centimeters; amount of liquid in tank, 200.0 milliliters.

Figure 5. - Concluded. Capillary rise in tube.

1-g configuration

Max.-height configuration

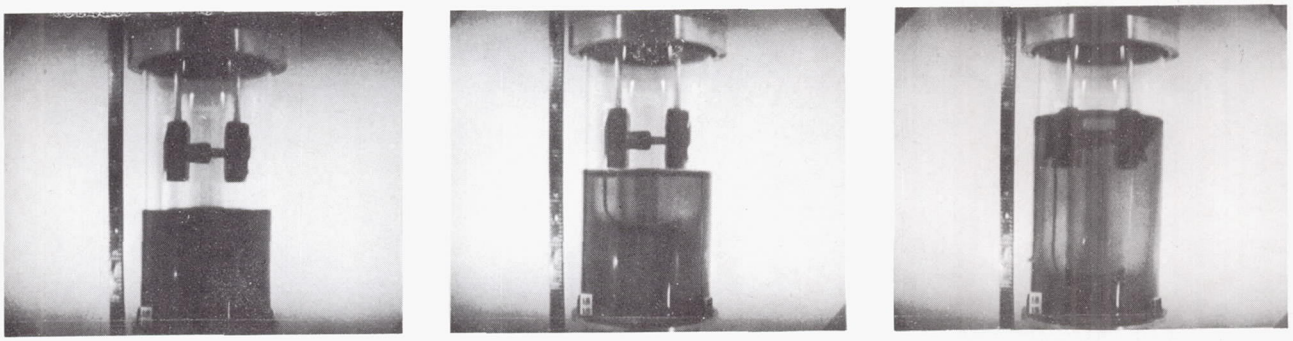

0 sec 1.06 sec 2.10 sec

(a) Tube diameter, 5.10 centimeters; amount of liquid in tank 228.7 milliliters.

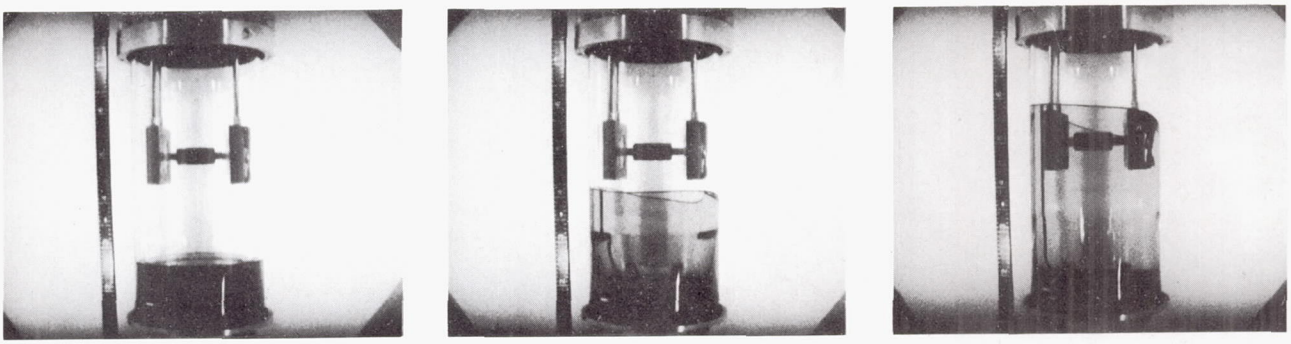

0 sec 0.69 sec 1.36 sec

(b) Tube diameter, 6.40 centimeters; amount of liquid in tank, 90.7 milliliters.

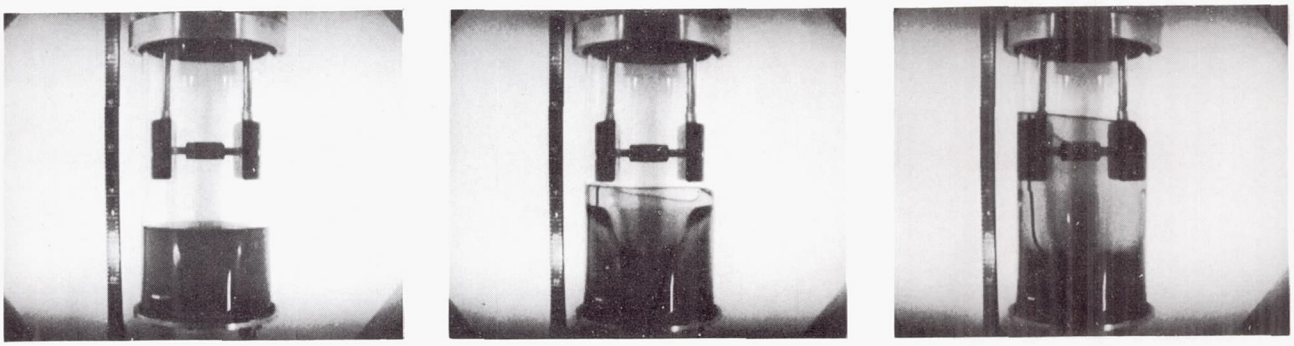

0 sec 0.54 sec 1.44 sec C-61702

(c) Tube diameter, 6.40 centimeters; amount of liquid in tank, 145.9 milliliters.

Figure 6. - Capillary rise in annular space.

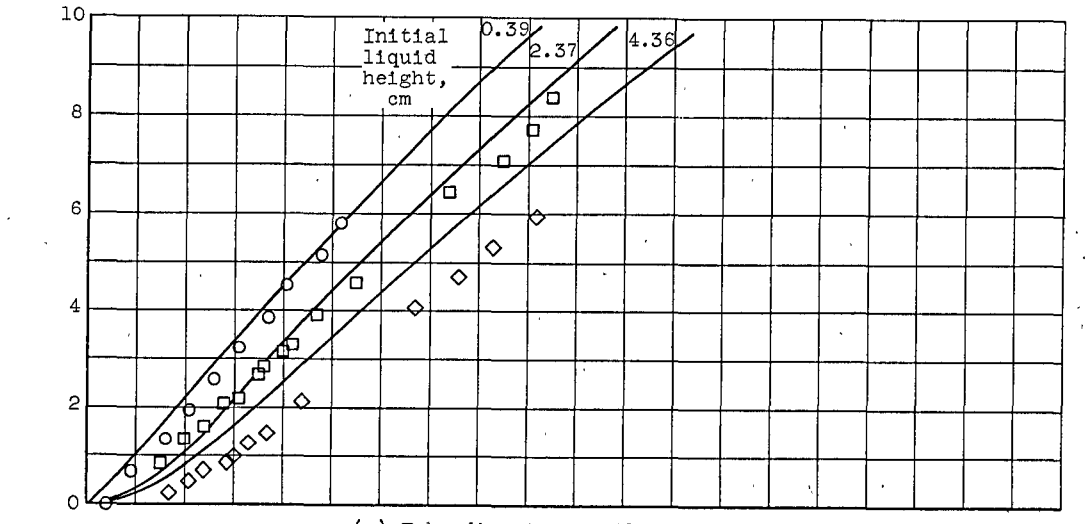

(a) Tube diameter, 0.48 centimeters.

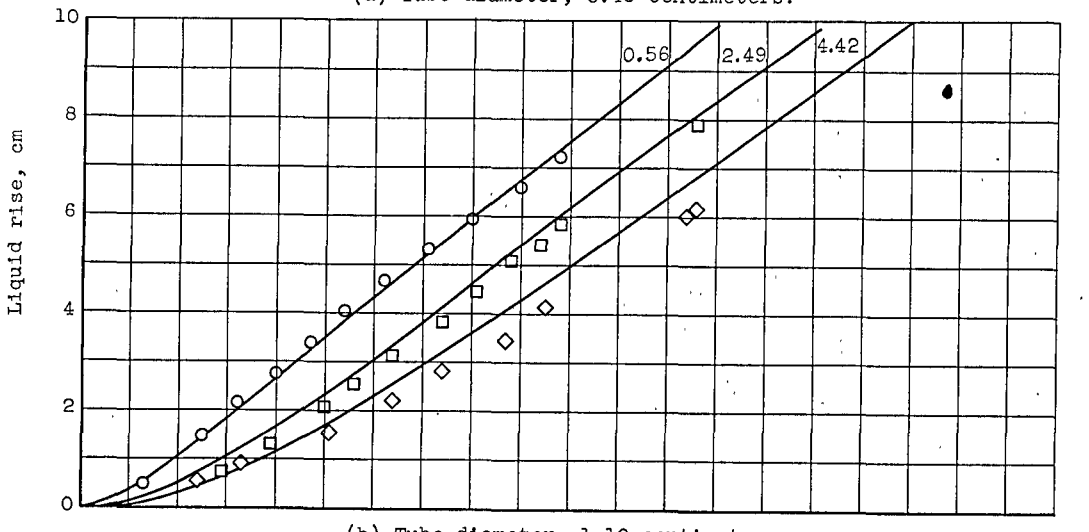

(b) Tube diameter, 1.10 centimeters.

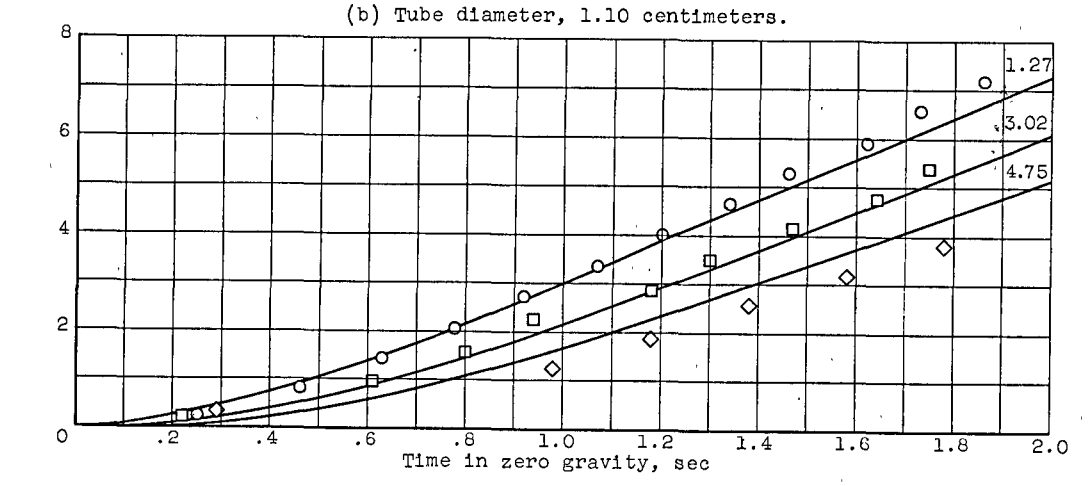

(c) Tube diameter, 2.20 centimeters.

Figure 7. - Variation of liquid rise in capillary tube as function of time in zero gravity.

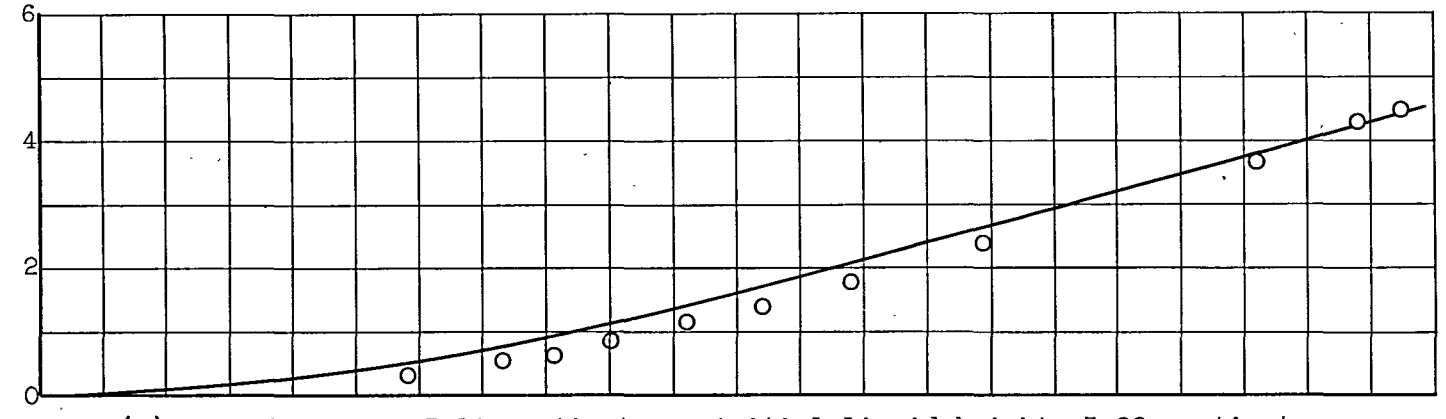

(a) Tube diameter, 5.10 centimeters; initial liquid height, 5.22 centimeters.

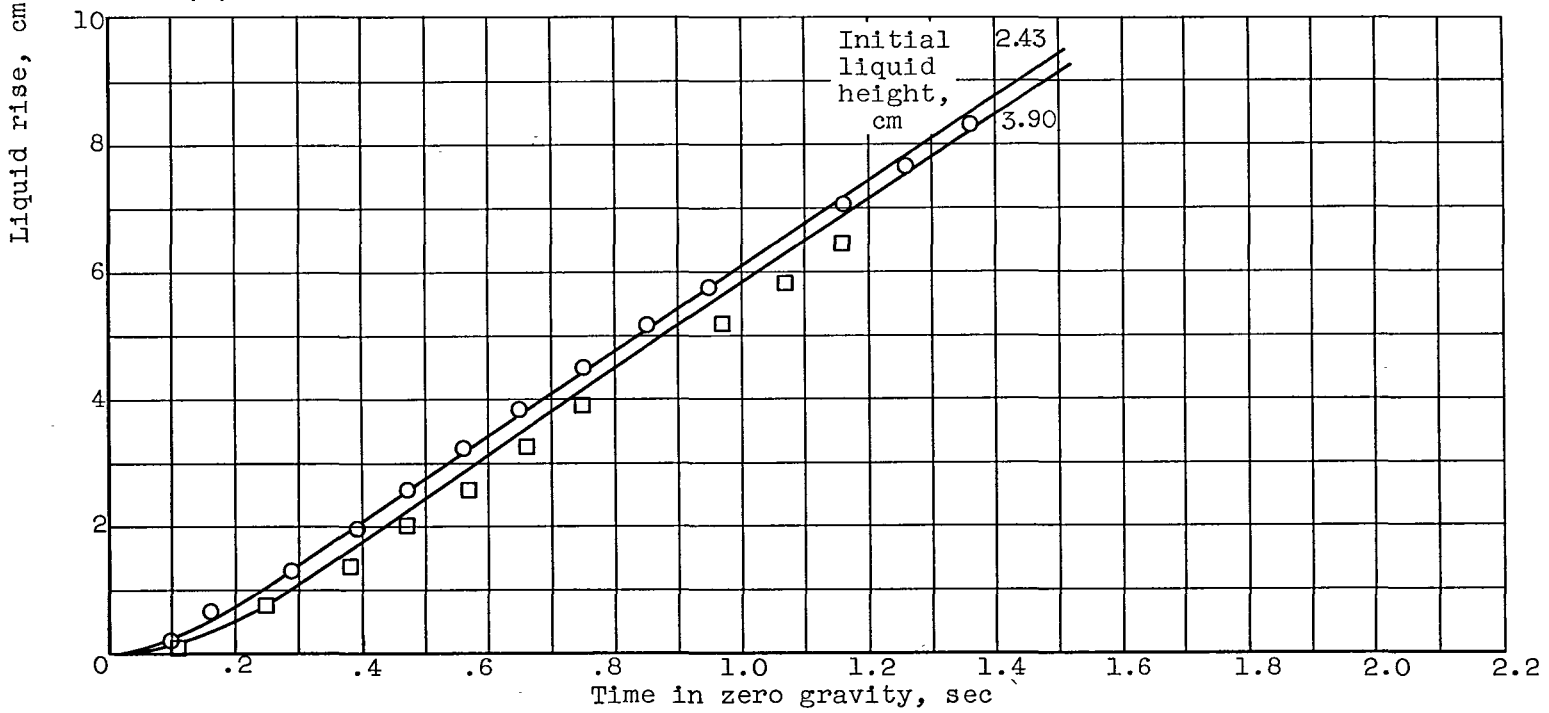

(b) Tube diameter, 6.40 centimeters.

Figure 8. - Variation of liquid rise in annular space as function of time in zero gravity.

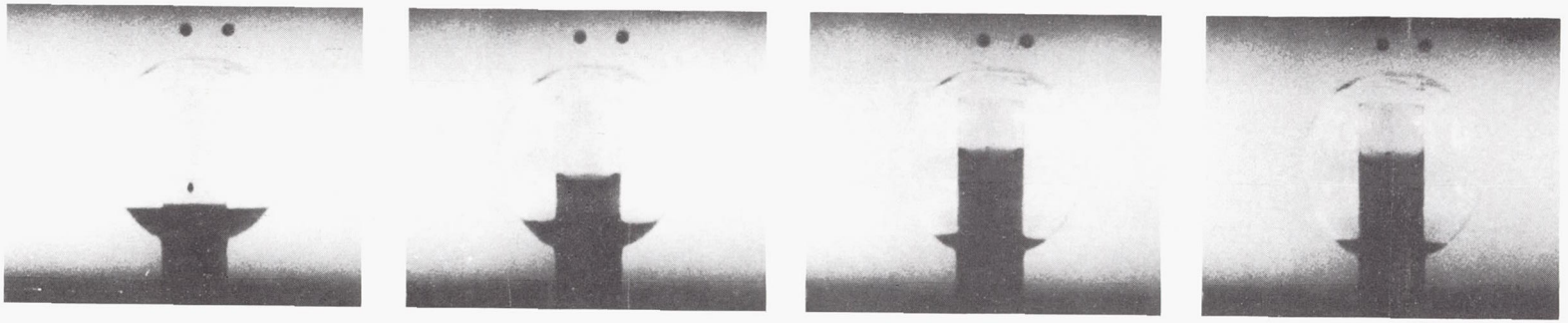

0 sec 0.51 sec 1.10 sec 2.21 sec

(a) Liquid- to tank-volume ratio, 10 percent.

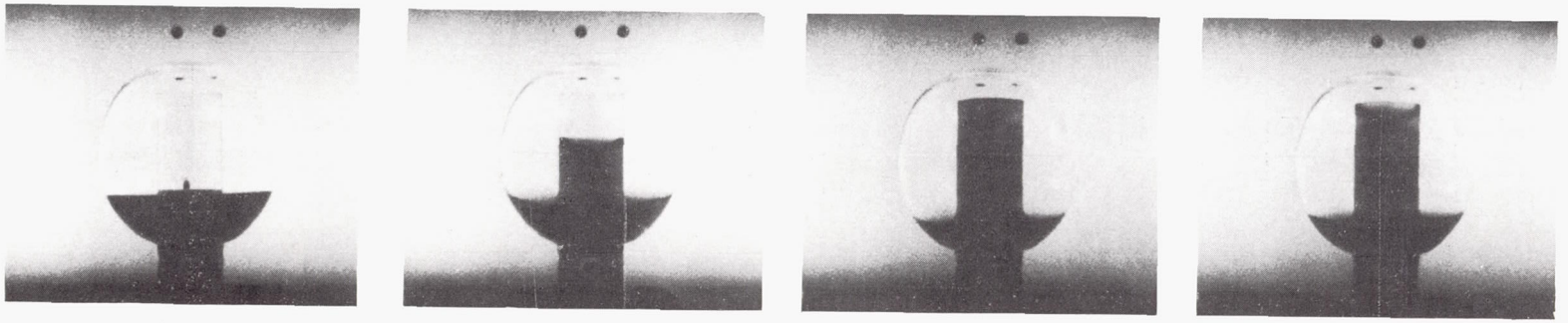

0 sec 0.49 sec 1.37 sec 2.19 sec

(b) Liquid- to tank-volume ratio, 20 percent.

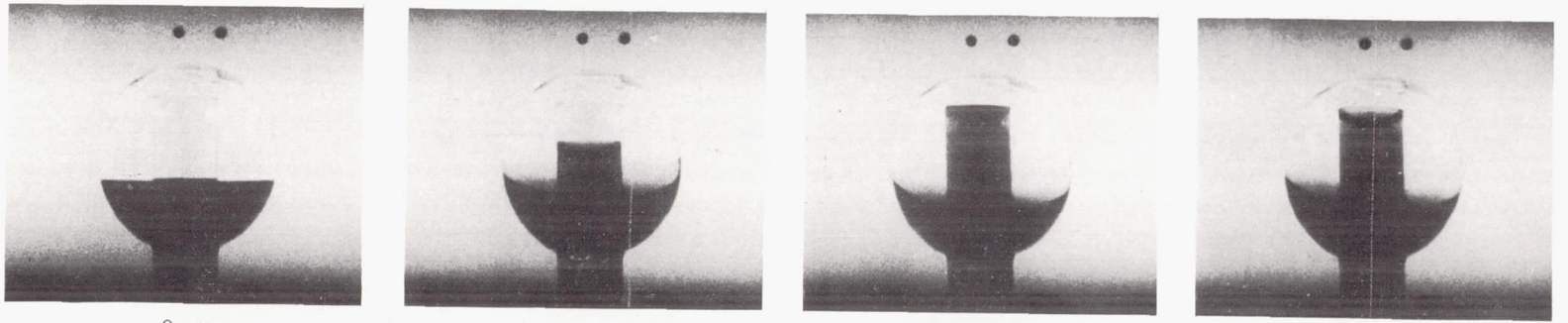

0 sec 0.64 sec 1.25 sec 2.25 sec C-61703

(c) Liquid- to tank-volume ratio, 30 percent.

Figure 9. - Liquid rise in 100-milliliter sphere with capillary surface-tension baffle over range of liquid- to tank-volume ratio.

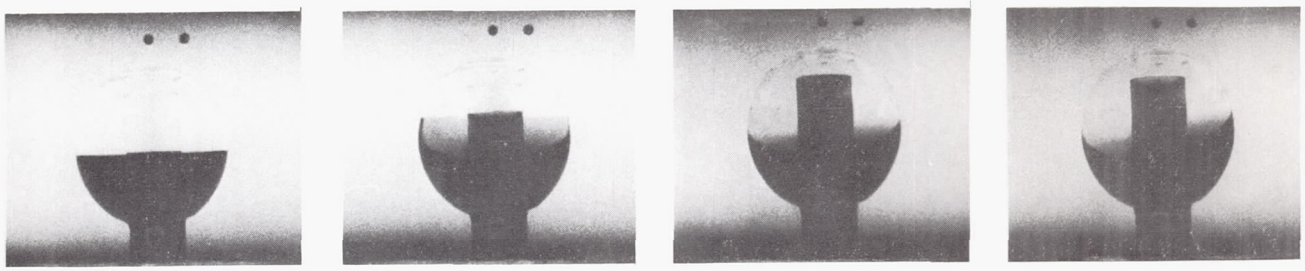

0 sec 0.57 sec 1.12 sec 2.20 sec

(d) Liquid- to tank-volume ratio, 40 percent.

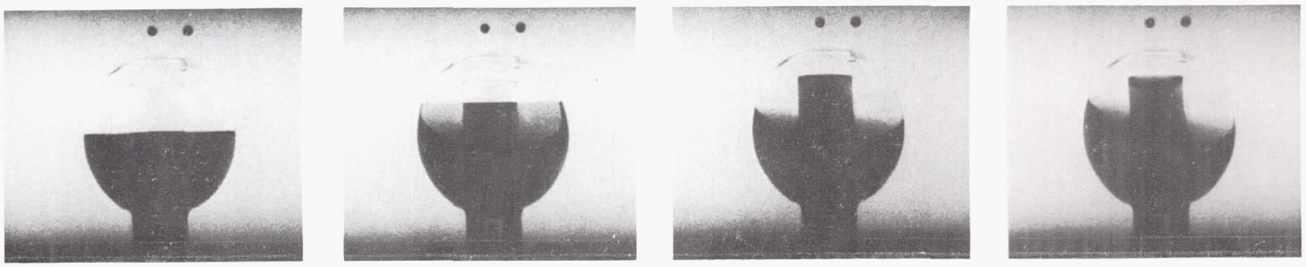

0 sec 0.52 sec 1.05 sec 2.19 sec

(e) Liquid- to tank-volume ratio, 50 percent.

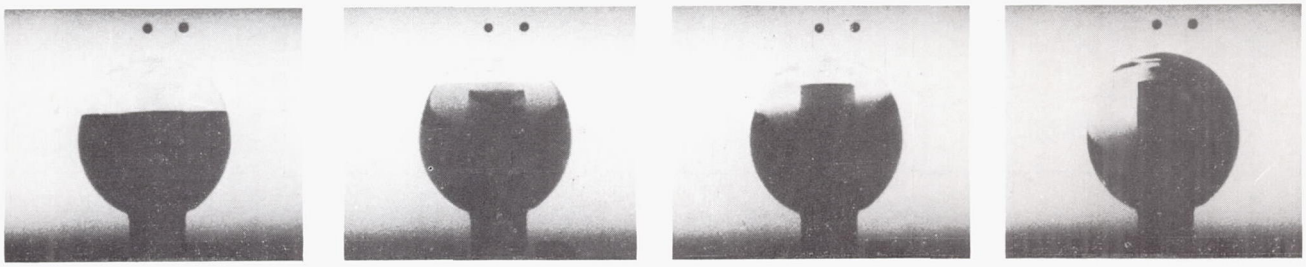

0 sec 0.46 sec 0.93 sec 2.14 sec

(f) Liquid- to tank-volume ratio, 70 percent.

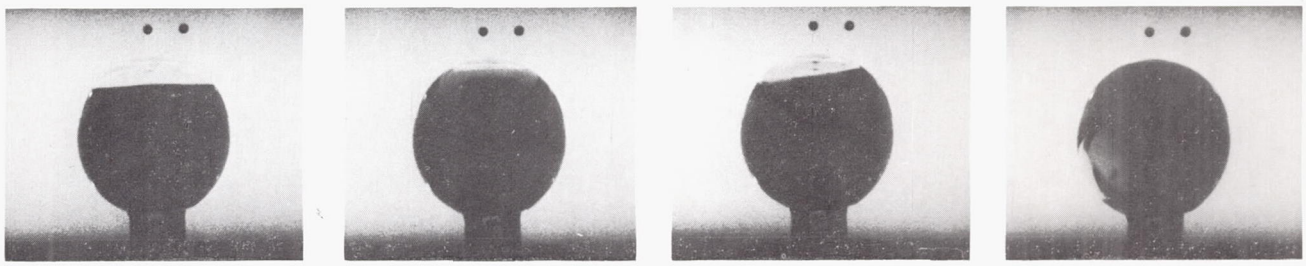

0 sec 0.30 sec 0.59 sec 2.27 sec C-61704

(g) Liquid- to tank-volume ratio, 90 percent.

Figure 9. - Concluded. Liquid rise in 100-milliliter sphere with capillary surface-tension baffle over range of liquid- to tank-volume ratio.

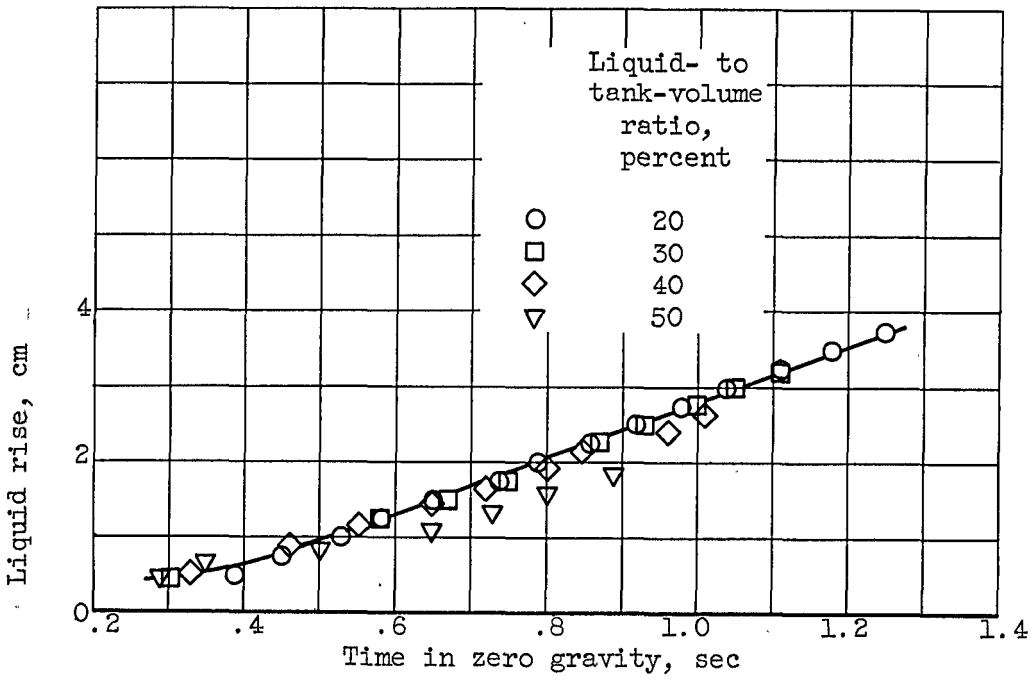

Figure 10. - Variation of liquid rise in capillary surface-tension baffle in spherical tank as function of time in zero gravity.

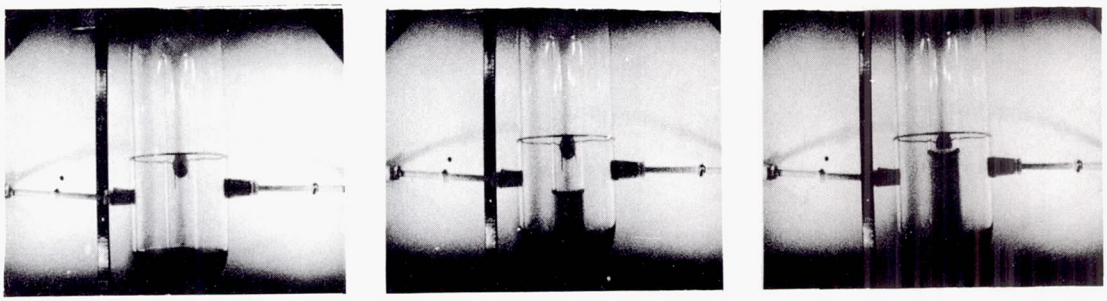

0 sec 1.19 sec 2.18 sec

(a) Liquid- to tank-volume ratio, 10 percent.

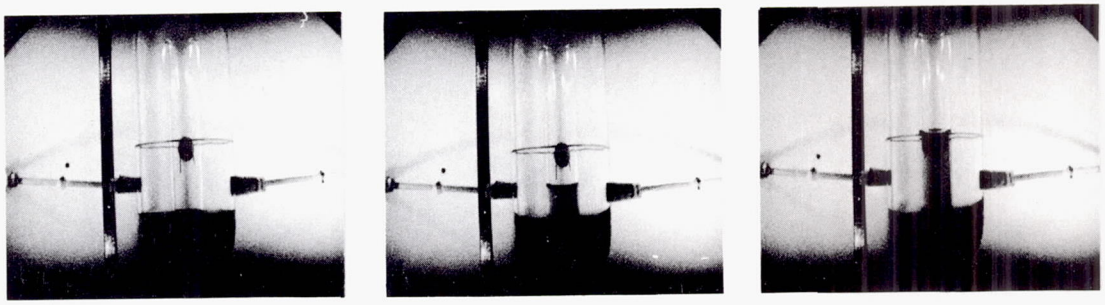

0 sec 1.13 sec 2.18 sec

(b) Liquid- to tank-volume ratio, 20 percent.

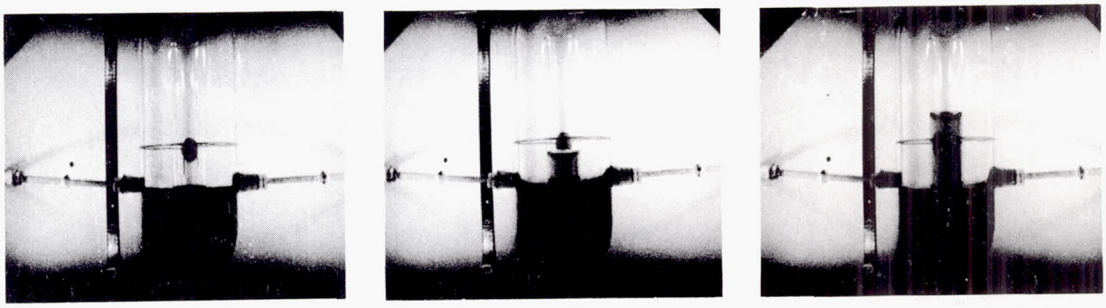

0 sec 1.14 sec 2.22 sec

(c) Liquid- to tank-volume ratio, 30 percent.

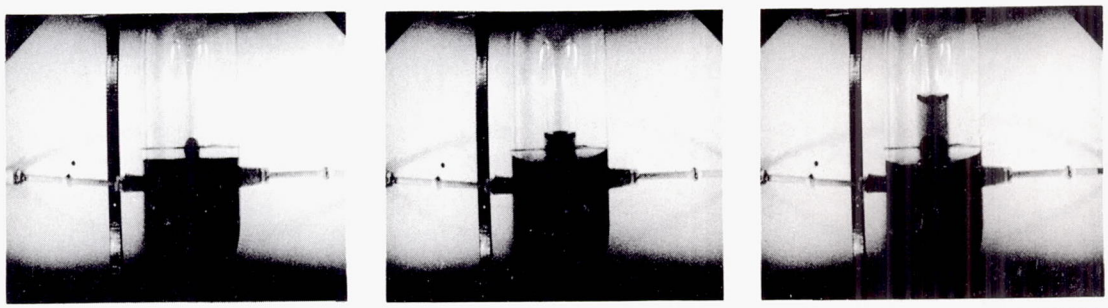

0 sec 1.44 sec 2.30 sec C-61705

(d) Liquid- to tank-volume ratio, 40 percent.

Figure 11. - Liquid rise in 440-milliliter cylinder with capillary surface-tension baffle over range of liquid- to tank-volume ratio.

1-g configuration

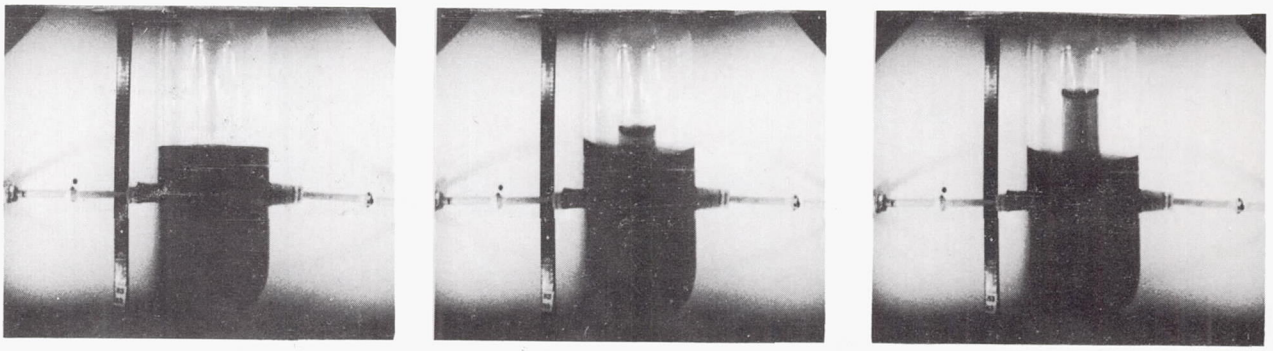

0 sec 1.16 sec 2.19 sec

(e) Liquid- to tank-volume ratio, 50 percent.

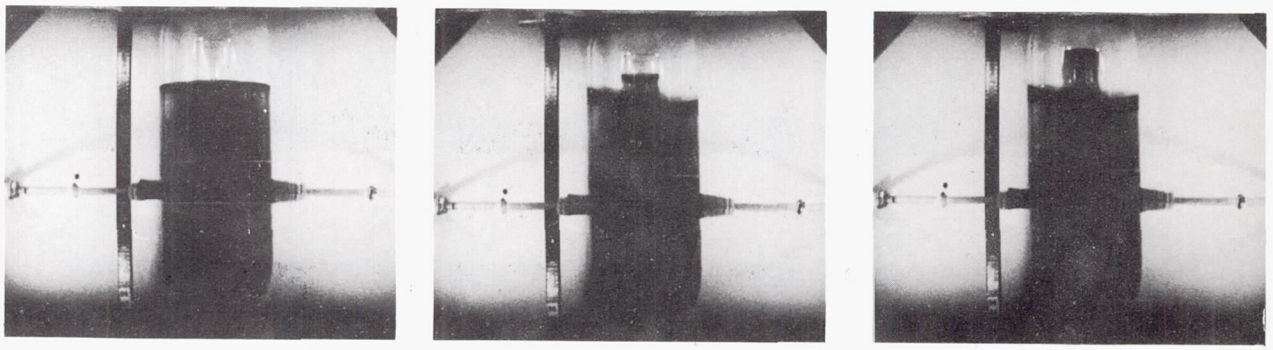

0 sec 1.35 sec 2.04 sec

(f) Liquid- to tank-volume ratio, 70 percent.

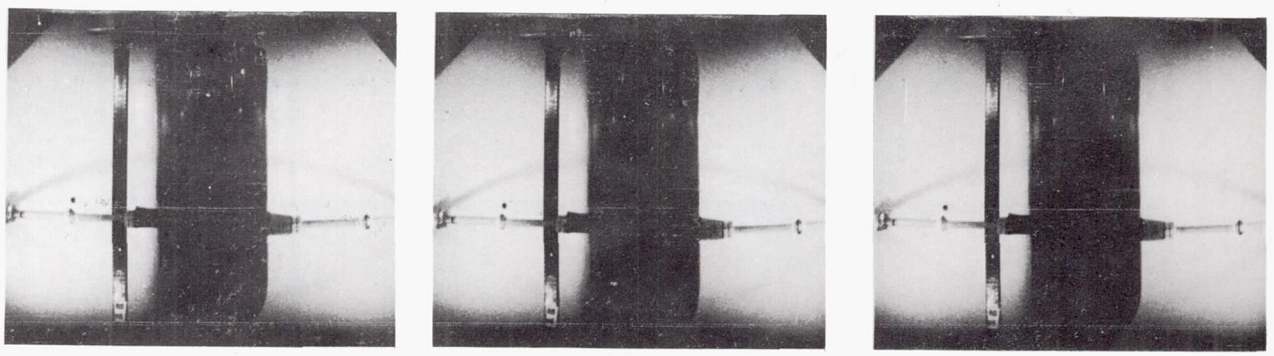

0 sec 1.13 sec 2.20 sec C-61706

(g) Liquid- to tank-volume ratio, 90 percent.

Figure 11. - Concluded. Liquid rise in 440-milliliter cylinder with capillary surface-tension baffle over range of liquid- to tank-volume ratio.

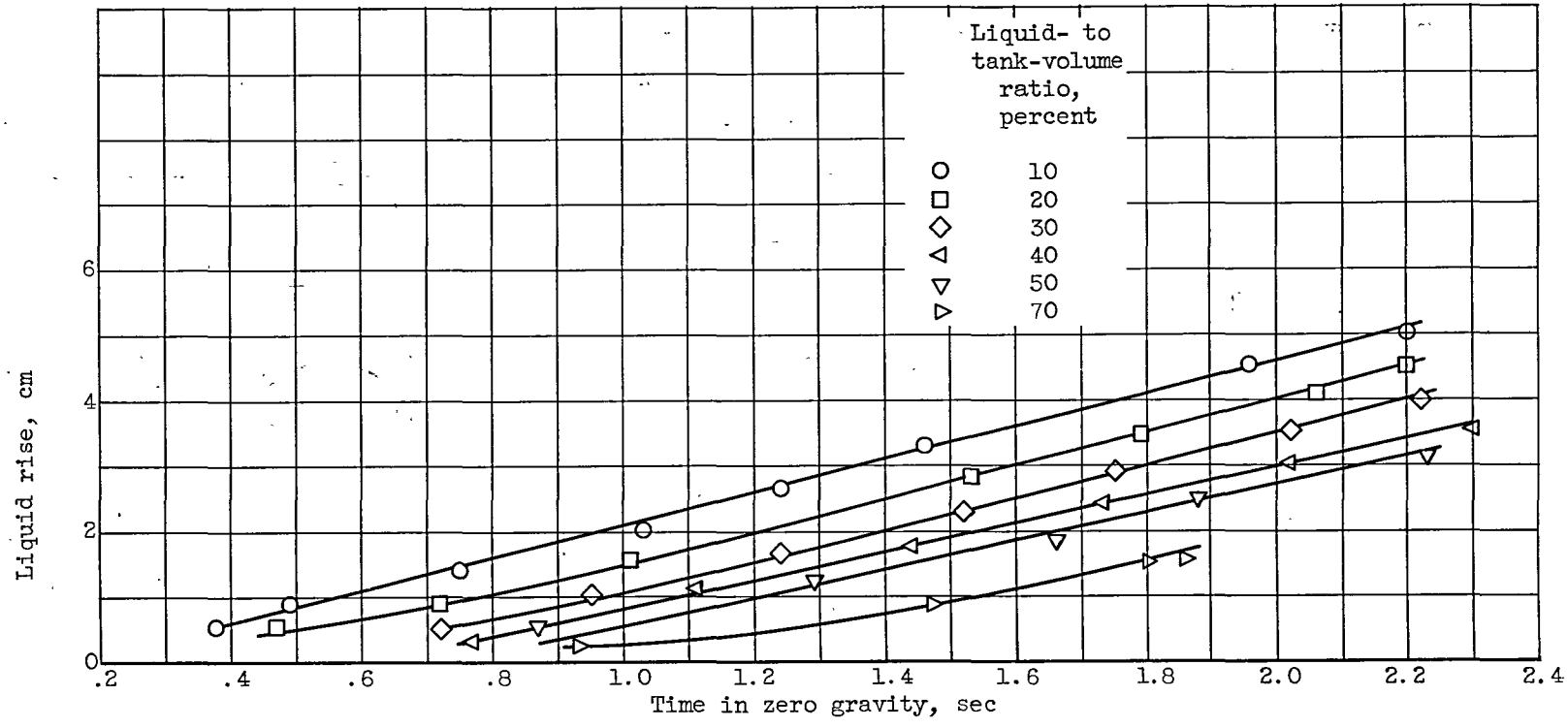

Figure 12. - Variation of liquid rise in capillary surface-tension baffle in cylindrical tank as function of time in zero gravity.

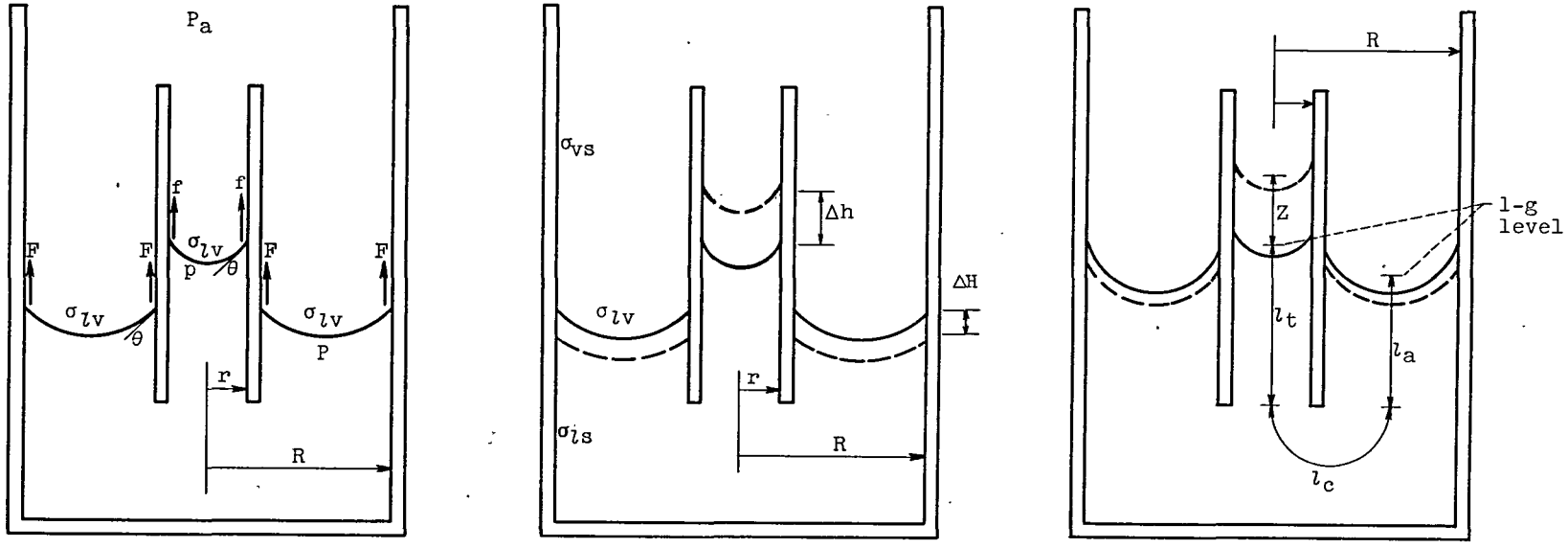

(a) Capillary-force parameters. (b) Surface-energy parameters. (c) Liquid-motion parameters.

Figure 13. - Sketch of capillary system under consideration showing system parameters.